# SAR-Analysis for Transmit SENSE with a 4-Channel Head Array at 3 T

**P. Ullmann[1], G. Wuebbeler[2], S. Junge[3], F. Seifert[2], W. Ruhm[3], J. Hennig[1]**

**[1]Department of Diagnostic Radiology, Medical Physics, University Hospital Freiburg, Freiburg, Germany, [2]Physikalisch-Technische Bundesanstalt, Berlin, Germany, [3]Bruker BioSpin MRI GmbH, Ettlingen, Germany**

**Introduction:** The concept of Transmit SENSE introduced by Katscher and Zhu [1,2] has gained considerable interest during the last few years and with the recently presented experimental implementations [3,4,5,6] the concept is now on the cusp of being evaluated for practical applications. However, one very important question, that has to be addressed when using phased array coils for simultaneous transmission with different waveforms on multiple channels, is the behavior of transmitted RF power and the specific absorption rate (SAR). In a previous study on this issue, Katscher et al. [7] showed for a certain array geometry that the RF power needed for Transmit SENSE pulses increases quadratically with the reduction factor, as long as the ratio $N/R$ ($N$: number of coils, $R$: reduction factor) is large. For small values of $N/R$ we face a very complex power behavior. In the present study the SAR behavior for Transmit SENSE with an existing 4-element array was analyzed, based on simulations of the electromagnetic fields, especially for this regime of small $N/R$ where no general rules of the SAR dependencies have been established so far.

**Materials and Methods:** The coil under consideration is a 4-element transmit-receive current-sheet-antenna (CSA) array [8,9] designed for $B_0$=3 T and loaded with a cylindrical water phantom (permittivity ε=76, conductivity σ=0.33 S/m) (Figure 1a). The opposite CSA-elements are separated by 25 cm and the phantom has a diameter of 19 cm. The electromagnetic properties were simulated in 3D using the XFDTD-software (REMCOM Inc.) and a good correspondence between simulated and measured data has already been shown in previous studies [8,9]. The pulses for 2D-selective excitation with Transmit SENSE were calculated based on the transmit sensitivities of a central axial slice (Figure 1b shows the normalized transmit sensitivity map of one single element). There was no excitation selectivity in the perpendicular direction. The pulses were calculated for different excitation patterns (flip angle 15°) in combination with both cartesian and spiral $k$-space trajectories and with a resolution of 40 x 40 points in the field-of-excitation (FOX). For the cartesian trajectory the approach from [1] was used. The pulses for the spiral trajectory were calculated according to [10] and Tikhonov regularization was applied. Afterwards SAR behavior within the whole phantom during the pulse was calculated based on the electric fields determined from the simulation (Figure 1c shows the normalized spatial SAR distribution of one single element). All calculations were performed in MATLAB (The MathWorks Inc., Natick, MA, USA).

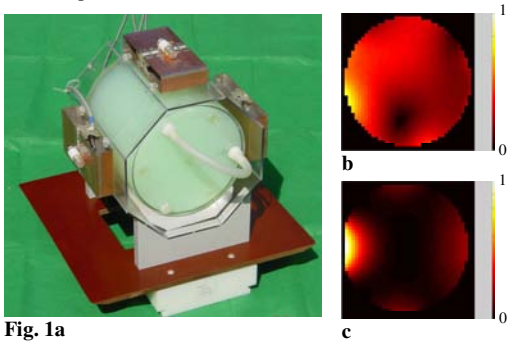

Fig. 1a

**Results:** The plots in Figure 2, 3 and 4 show the spatial distribution of the specific absorbed energy for a central axial slice when exciting different patterns using Transmit SENSE pulses with reduction factors of 1, 2 and 4. It can be seen that this distribution strongly depends on the selected pattern and even more on the used reduction factor. Even though the maximum absorbed energy in these cases is found in the vicinity of the antennas, which may change fundamentally with different geometries and field strengths, the concentration of the energy at the different antennas is very variable and sometimes perhaps even not according to expectations as in Fig. 3d.

In Tab. 1 numerical values of the total pulse energy applied to the coil elements during a Transmit SENSE pulse and the calculated total absorbed energy in the phantom are displayed. Furthermore the ratio between the local maximum and the spatial average of the SAR is listed. The data shows a moderate increase of the absorbed power when moving from $R$=1 to $R$=2 and a dramatic rise for $R$=4. This is an indication that the setup operates at its limit in this case, and the strong increase of pulse energy can be understood as an analogy to noise amplification caused by the $g$-factor in "receive SENSE" [11]. It is interesting to note, that the absorbed power has not necessarily the same dependence from $R$ as the applied pulse power due to the individual phase behavior of the array elements. The data further shows that the target pattern and the selected $k$-space trajectory strongly influence not only the spatial distribution but also the absolute value of the absorbed energy. E.g. when exciting a homogeneous pattern in the image, the corresponding $k$-space pattern is strongly localized in the center. With a cartesian trajectory this leads to excitation pulses with few, relatively tall peaks that have a high pulse energy. In the spiral case, where the trajectory stronger weights the $k$-space center the pulse energy is much lower. Is has to be noted that e.g. these pulses for homogeneous excitation with these very sharp peaks may lead to experimental problems since they are very sensitive to imperfections, despite the fact that they are numerically correct. Another important aspect shown in the data is that for the given setup the ratio between the local maximum of SAR and the spatial average is also very variable. There can be significant concentration of absorbed energy at certain places despite a moderate spatial average of the SAR.

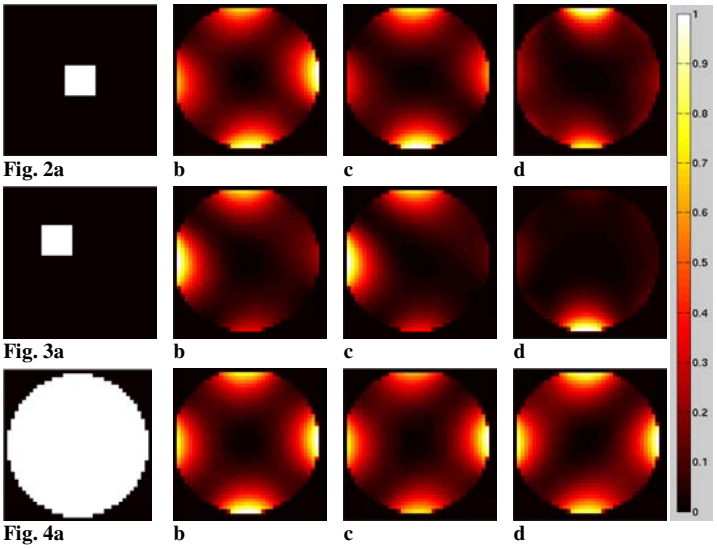

Fig. 2a b c d

Fig. 3a b c d

Fig. 4a b c d

Spatial distribution of the absorbed energy for different excitation patterns and reduction factors $R$ with a cartesian trajectory and undersampling in L-R direction. (a: target excitation pattern; b,c,d: absorbed energy for $R$=1,2,4 (all maps are in arbitrary units and individually scaled to the range [0 1]).

| Pattern | centered square | | | | | | off-centered square | | | | | | homogeneous excitation | | | | | |
|---|---|---|---|---|---|---|---|---|---|---|---|---|---|---|---|---|---|---|
| Trajectory | cartesian | | | spiral | | | cartesian | | | spiral | | | cartesian | | | spiral | | |
| Reduction factor | 1 | 2 | 4 | 1 | 2 | 4 | 1 | 2 | 4 | 1 | 2 | 4 | 1 | 2 | 4 | 1 | 2 | 4 |
| Pulse length [ms] | 12.53 | 6.26 | 3.13 | 12.53 | 6.26 | 3.13 | 12.53 | 6.26 | 3.13 | 12.53 | 6.26 | 3.13 | 12.53 | 6.26 | 3.13 | 12.53 | 6.26 | 3.13 |
| Pulse energy [mJ] | 3.80 | 9.44 | 593.67 | 1.14 | 2.75 | 164.69 | 3.73 | 8.07 | 622.77 | 1.12 | 2.63 | 96.70 | 55.27 | 110.69 | 294.23 | 3.34 | 8.58 | 137.49 |
| Absorbed energy [mJ] | 2.69 | 6.19 | 105.79 | 0.79 | 1.73 | 29.63 | 2.42 | 5.03 | 122.47 | 0.71 | 1.58 | 29.50 | 34.40 | 69.56 | 150.84 | 2.07 | 5.12 | 57.47 |
| Ratio maximum local / average SAR | 6.55 | 8.32 | 10.70 | 6.59 | 7.10 | 7.15 | 9.75 | 10.46 | 20.48 | 9.49 | 10.00 | 8.14 | 6.70 | 7.44 | 6.38 | 6.73 | 6.23 | 11.19 |

**Tab. 1**: Transmitted and absorbed energy for different excitation patterns, $k$-space trajectories and reduction factors.

**Discussion and conclusions:** The results of this study indicate clearly, that in the regime of small $N/R$ a very detailed analysis of SAR is necessary for performing Transmit SENSE excitation since there is a very complex interdependence between excitation pattern, used k-space trajectory, coil geometry and reduction factor that strongly influences the global amount and the spatial distribution of the absorbed energy. Even details of the algorithm may play a significant role such a regularization, especially for the case $N$=$R$. This clearly demonstrates the need for a detailed safety analysis that has to be individually adapted to the setup and the calculation methods used for the Transmit SENSE experiments. Even for the case of large $N/R$, where previous studies have found a quadratic power behavior (see [7]), is has to be analyzed if this regular dependence holds for different geometrical setups and pulse calculation methods and how the SAR is distributed within the object.

**References:** [1] U. Katscher et al., Magn. Reson. Med. 49:144-150 (2003); [2] Y. Zhu, Magn. Reson. Med. 51:775-764 (2004); [3] P. Ullmann et al., Magn. Reson. Med. 54:994-1001 (2005); [4] P. Ullmann et. al., Proc. ISMRM 2005, p.15; [5] Y. Zhu et al., Proc. ISMRM 2005, p.14; [6] P. Ullmann et al., Proc. ESMRMB 2005, 186; [7] Katscher et al., Proc. ISMRM 2005, p.17; [8] S. Junge et al., Proc. ISMRM 2004, p. 41; [9] Wuebbeler et al., Proc. ISMRM 2004, p. 665; [10] W. Grissom et al., Proc. ISMRM 2005, p. 19; [11] K. Pruessmann et al., Magn. Reson. Med. 42:952-962 (1999).